Towards Efficient EM Wave Manipulation Using a Discrete Dielectric Huygens' Metasurface

Abhishek Sharma, Alex M. H. Wong
State Key Laboratory of Terahertz and Millimeter Waves
Department of Electrical Engineering
City University of Hong Kong, Hong Kong SAR, China
abhisheksharma.rf@gmail.com, alex.mh.wong@cityu.edu.hk

Abstract—This paper presents a spatially varying discrete dielectric Huygens' metasurface (DD-HMS) that achieves beam splitting. The proposed structure consists of two elements per grating period and the phase difference between neighbouring elements is 180°. The resultant bipartite Huygens' metasurface leads to a simplified, robust and cost-effective design as compared to finely discretized metasurfaces. A 2D full-wave Floquet simulation demonstrates that the proposed metasurface splits the normal incident plane wave into different directions according to the generalized Snell's law, and contains over 80% of the transmitted power.

Index Terms—beam splitter, bipartite Huygens' metasurface, discrete dielectric Huygens' metasurface.

I. INTRODUCTION

The electromagnetic (EM) wave manipulation has been the subject of intense research over the decades in both microwave and the optical regime. The introduction of 2D analogues of metamaterials, known as *metasurfaces*, has revolutionized the field of surface electromagnetics, which opens up the whole new way of manipulating EM waves, almost at will [1], [2]. However, most of the metasurfaces provide electric response to the incoming EM waves, which limit their ability to fully control the wavefronts.

More recently, Huygens' metasurface (HMS) has gained much attention for their ultimate wave manipulation capabilities [3], [4], which opens new avenues for transforming EM waves. The HMS is fundamentally based on the surface equivalence principle, and comprises collocated electric and magnetic polarizable particles, which provide both electric and magnetic responses to an incoming EM wave, leading to full control with great flexibility and high efficiency. Over the past lustrum, the HMS have impressively demonstrated several novel phenomena such as anomalous reflection/refraction [5]–[7], retroreflection [8], beam splitting [9], [10], and antenna gain enhancement [11], to name a few.

In general, the HMS can be constructed either by using cascaded multilayer structure [5] or by wire-loop configuration [12]. This requirement may lead to fabrication difficulties, especially in the millimeter-wave (mm-w) frequency regime and beyond. In addition, the inevitable ohmic losses associated with the metallic structures degrade the performance in the higher frequency spectrum. To alleviate these drawbacks, the concept of dielectric metasurface has been suggested as a promising route for extraordinary EM wave manipulation [13]. The dielectric metasurface consists of low-loss dielectric resonator (DR), capable of providing both electric and magnetic responses [14]. In addition, by fine-tuning the geometrical parameters of the DR, it is possible to overlap the electric and magnetic dipole modes, thereby realizing the dielectric Huygens' surfaces with high-transmission and full 360° phase coverage [15]. Relatively very limited work on dielectric Huygens' metasurfaces has been reported [16]–[21], and the majority of them were limited to the optical regime, leaving the mm-wave regime bit unexplored.

In this paper, we present a beam splitter based on the discrete dielectric Huygens' metasurface (DD-HMS) in the millimeter-wave (mm-w) frequency spectrum. To the best knowledge of the authors, such discrete dielectric Huygens' metasurface is not presented in the literature earlier. The beam splitting here is achieved by employing two elements per grating period, with the phase difference of 180°. The resultant structure is termed as bipartite dielectric Huygens' metasurface, which may lead to simplified, robust and cost-effective design. Additionally, this kind of discrete metasurface may relax the fabrication difficulties which may arise in the mm-w frequency range and beyond.

II. UNIT-CELL DESIGN

Fig. 1(a) shows a typical simulation environment to characterize the unit cell. A cylindrical dielectric meta-atom of radius R, height H and $\epsilon_r = 6.15$ is placed at the origin of the simulation domain, with periodic boundaries set at the planes $x = \pm U_x/2$ and $y = \pm U_y/2$. We first study the resonant behaviour of the dielectric cylinder, and for this purpose, we have chosen the dimensions as $R = 1.4$ mm, $H = 1$ mm and $U_x = U_y = 3.6$ mm. A TE polarized plane wave (electric field oriented along the x-direction) is incident normally from the port 1, and the transmission spectrum is studied. The two transmission dips is observed in Fig. 1(b), one at 60.6 GHz and other at 65.6 GHz. On analyzing the electric field distribution at these frequencies (Figs. 1(c) and 1(d)), it can be concluded that at 60.6 GHz, the electric field resembles that of an electric dipole pointing along x-axis, whereas at 65.6 GHz, it resembles that of the magnetic dipole oriented along y-axis.

Next, to realize the dielectric Huygens' metasurface (D-HMS), we have tuned the geometrical parameters associated with the DR geometry such that both the resonances get overlapped, providing high transmission and 2π phase coverage. The dimension of the DR corresponding to this case is- $R = 1.3$ mm and $H = 1.25$ mm. The transmission spectrum of the D-HMS is depicted in Fig. 2. As expected, the resultant D-HMS features the transmission greater than 0.85 along with the full 2π phase coverage over the frequency range of 50-70 GHz.
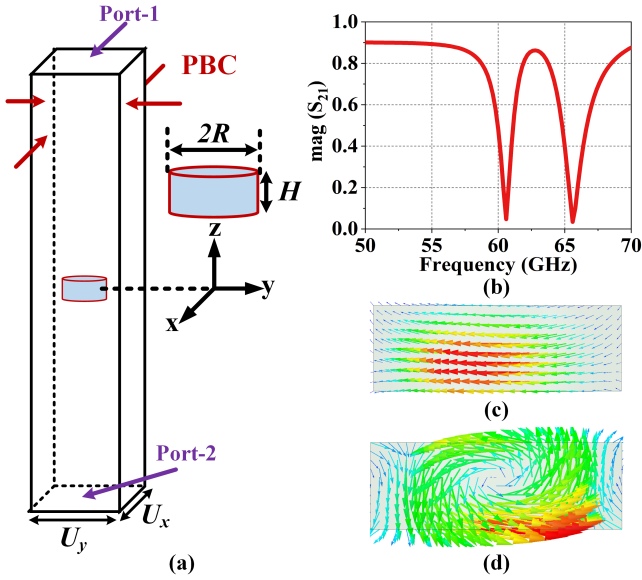
Fig. 1. (a) Typical simulation environment with periodic boundary conditions (PBC) and Floquet ports (Port-1 and Port-2). (b) Simulated magnitude of the transmission coefficient for $R = 1.4$ mm and $H = 1.25$ mm. (c) Electric field distribution at 60.6 GHz. (d) Electric field distribution at 65.6 GHz.
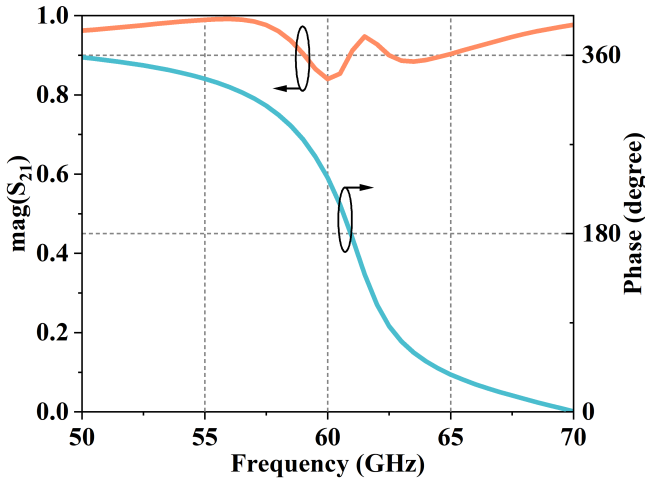

Fig. 2. Simulated magnitude and phase of the transmission coefficient for $R = 1.3$ mm and $H = 1.25$mm.

III. REALIZATION OF BEAM-SPLITTER

For the illustration of the beam splitter, a linear phase-gradient D-HMS is designed by placing two elements side-by-side per grating period. As initial dimensions, two sets of R and H are chosen to have 180° phase difference between them. The supercell thus created is simulated using periodic boundary conditions and floquet ports. In this new simulation environment, the combined elements behave bit differently due to the mutual coupling dynamics, and thus need re-optimization. The optimized dimensions of DR are $R_1 = 1.35$ mm, $H_1 = 1.35$ mm, $R_2 = 1.15$ mm, and $H_2 = 1.15$ mm. In addition, due to the periodicity of the boundary conditions, three floquet modes (0th mode, +1 mode and -1 mode) are allowed to exist in the simulation domain. Fig. 3(a) shows the simulated magnitude of the transmission modes for one period of the metasurface. From the figure, it is clear that at the frequency of interest (61.5 GHz), the transmission of the +1 mode and -1 mode is
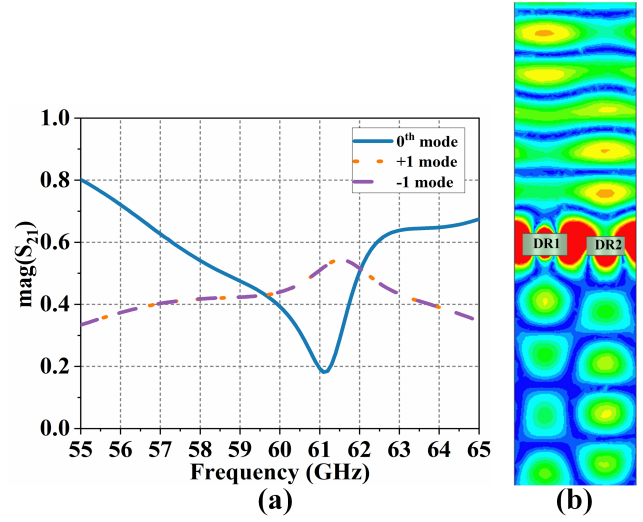

Fig. 3. (a) Simulated magnitude of the transmission coefficient of the metsurface. (b) Electric field distribution showing the interference pattern of the two splitted beams at the transmission side.

maximum, whereas the 0th mode which corresponds to plane wave at 0° is suppressed.

The deflected angle can be calculated using the generalized Snell's law [2]

$$n_t \sin \theta_t - n_i \sin \theta_i = \frac{\lambda_0}{2\pi} \frac{d\Phi}{dy} \qquad (1)$$

where, n_t and n_i are the refractive index of incident and transmitted medium, θ_i and θ_t are the incident and transmitted angle, λ_0 is the free space wavelength, $d\Phi$ is the phase difference between the successive unit cells and dy is the period of unit cell. Since the phase gradients along the $+x$ and $-x$ directions are same, thus a normally incident plane wave ($\mathbf{k_i}$) is splitted in two directions-($\mathbf{k_{t,1}}$) and ($\mathbf{k_{t,-1}}$), at an angle $\pm 41.8°$ with respect to the normal (z-axis) having equal amplitude. For better clarity and visualization of beam splitting, two supercells of the metasurface is also simulated and the result is presented in Fig. 4.

We have demonstrated through simulations, a proof-of-concept of beam splitting based on the bipartite dielectric Huygens' metasurface. For the practical realization, a deep subwavelength supporting substrate can be added without affecting the overall performance. Besides, the additive manufacturing technique, popularly known as 3D printing, can be employed to fabricate the proposed metasurface.

IV. CONCLUSION

In this paper, we have reported the first investigation on the spatially varying dielectric Huygens' metasurface–comprising smaller number of elements per metasurface period, which open new prospects for extreme EM wave manipulation. As a proof-of-concept, we have presented a beam splitter, comprising only two elements per grating period. It has been shown through full-wave simulations that the resultant metasurface splits the normal incident plane wave in two directions, angles at $\pm 41.8°$ with respect to the normal, and contains over 80% of the transmitted power. The proposed bipartite Huygens' metasurface may lead to simplified, robust and cost-effective design as compared to finely discretized counterparts.
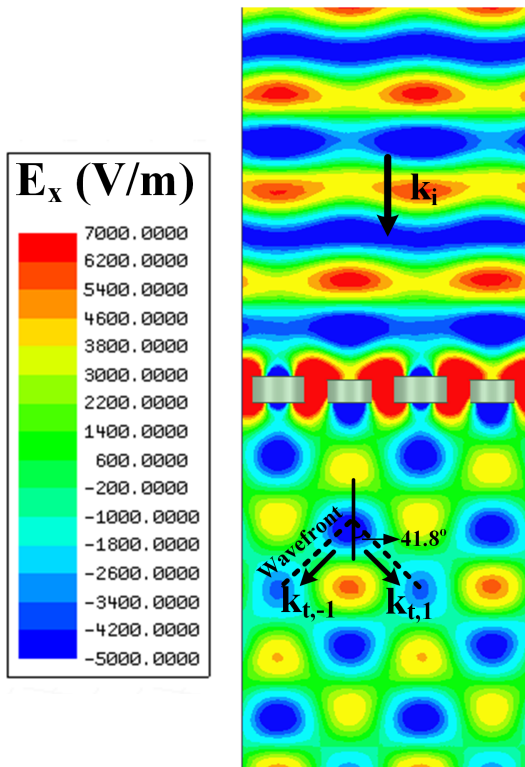
Fig. 4. Electric field distribution showing the interference pattern of the two splitted beams at the transmission side.

REFERENCES

[1] Oscar Quevedo-Teruel *et al.*, "Roadmap on metasurfaces," *J. Opt.*, **21**, 073002, 2019.

[2] S. Sun *et al.*, "Electromagnetic metasurfaces: physics and applications," *Adv. Opt. Photon.*, **11**, pp. 380-479, 2019.

[3] Ariel Epstein and George V. Eleftheriades, "Huygens' metasurfaces via the equivalence principle: design and applications," *J. Opt. Soc. Am. B*, **33**, pp. A31-A50, 2016.

[4] Michael Chen, Minseok Kim, Alex M.H. Wong, and George V. Eleftheriades, "Huygens' metasurfaces from microwaves to optics: a review," *Nanophotonics*, **7**, pp. 1207-1231, 2018.

[5] Michael Chen, Elena Abdo-Sánchez, Ariel Epstein, and George V. Eleftheriades, "Theory, design, and experimental verification of a reflectionless bianisotropic Huygens' metasurface for wide-angle refraction," *Phys. Rev. B*, **97**, 125433, 2018.

[6] Alex M. H. Wong and George V. Eleftheriades, "Perfect Anomalous Reflection with a Bipartite Huygens' Metasurface," *Phys. Rev. X*, **8**, 011036, 2018.

[7] C. Qi and Alex M. H. Wong, "A coarsely discretized Huygens' metasurface for anomalous transmission," accepted for presentation in *2019 Asia-Pacific Microwave Conference*, to be held in Singapore, Dec. 2019.

[8] Alex M. H. Wong, Philip Christian and George V. Eleftheriades, "Binary Huygens' Metasurfaces: Experimental Demonstration of Simple and Efficient Near-Grazing Retroreflectors for TE and TM Polarizations," *IEEE Trans. Antennas Propag.*, **66**, pp. 2892-2903, 2018.

[9] Minseok Kim, Alex M. H. Wong, and George V. Eleftheriades, "Optical Huygens'Metasurfaces with Independent Control of the Magnitude and Phase of the Local Reflection Coefficients," *Phys. Rev. X*, **4**, 041042, 2014.

[10] S. Jia, X. Wan, D. Bao, Y. Zhao, and T. J. Cui, "Independent controls of orthogonally polarized transmitted waves using a Huygens metasurface," *Laser & Photonics Reviews*, **9**, pp. 545-553, 2015.

[11] Michael Chen, Ariel Epstein, and George V. Eleftheriades, "Design and Experimental Verification of a Passive Huygens' Metasurface Lens for Gain Enhancement of Frequency-Scanning Slotted-Waveguide Antennas," *IEEE Trans. Antennas Propag.*, **67**, pp. 4678-4692, 2019.

[12] C. Pfeiffer and A. Grbic, "Metamaterial Huygens' Surfaces: Tailoring Wave Fronts with Reflectionless Sheets," *Phys. Rev. Lett.*, **110**, 197401, 2013.

[13] Seyedeh Mahsa Kamali, Ehsan Arbabi, Amir Arbabi, and Andrei Faraon, "A review of dielectric optical metasurfaces for wavefront control," *Nanophotonics*, **7**, pp. 1041-1068, 2018.

[14] Isabelle Staude *et al.*, "Tailoring Directional Scattering through Magnetic and Electric Resonances in Subwavelength Silicon Nanodisks," *ACS Nano*, **7**, pp. 7824-7832, 2013.

[15] Manuel Decker *et al.*, "High-Efficiency Dielectric Huygens' Surfaces," *Adv. Optical Mater.*, **3**, pp. 813–820, 2015.

[16] Mikhail I. Shalaev *et al.*, "High-efficiency all-dielectric metasurfaces for ultracompact beam manipulation in transmission mode," *Nano Lett.*, **15**, pp. 6261-6266, 2015.

[17] Wenyu Zhao *et al.*, "Dielectric Huygens' Metasurface for High Efficiency Hologram Operating in Transmission Mode," *Scientific Reports*, **6**, 30613, 2016.

[18] Katie E. Chong *et al.*, "Efficient Polarization-Insensitive Complex Wavefront Control Using Huygens' Metasurfaces Based on Dielectric Resonant Meta-atoms," *ACS Photonics*, **3**, pp. 514-519, 2016.

[19] Zhongyi Guo, Lie Zhu, Kai Guo, Fei Shen and Zhiping Yin, "High-Order Dielectric Metasurfaces for High-Efficiency Polarization Beam Splitters and Optical Vortex Generators," *Nanoscale Research Letters*, **12**, 2017.

[20] K. Achouri, A. Yahyaoui, S. Gupta, H. Rmili and C. Caloz, "Dielectric Resonator Metasurface for Dispersion Engineering," *IEEE Trans. Antennas Propag.*, **65**, pp. 673-680, 2017.

[21] Adam J. Ollanik *et al.*, "High-Efficiency All-Dielectric Huygens Metasurfaces from the Ultraviolet to the Infrared," *ACS Photonics*, **5**, pp. 1351-1358, 2018.